Coke Effect in Mass Transport and Morphology of Pt-Al_2O_3 and Ni-Mo-Al_2O_3 Catalysts

F. García-Ochoa and A. Santos
Dept. Ingeniería Química, Universidad Complutense, 28040-Madrid, Spain

The effect of high levels of coke deposit on catalyst properties and mass transport through the pores space was studied using commercial catalysts, Pt-Al_2O_3 and Ni-Mo-Al_2O_3. Changes in porosity, pore-size distribution and internal surface area of several aged catalysts were compared to those of fresh catalyst. Effective diffusivity was also measured by pulse chromatography. For Pt-Al_2O_3, which shows a high initial porosity (0.93) and a relative high mean pore radius (300 Å), catalyst properties remain unchanged while coke content increased. For the Ni-Mo-Al_2O_3 catalyst (with initial porosity of 0.53 and mean pore radius of 50 Å), however, with an increase of 15% in coke content, isolated void regions appear, and porosity, internal surface area and effective diffusivity decrease sharply. Pore and stochastic models were used to interpret the effective diffusivity experimentally measured. A structural parameter in each case, tortuosity factor in pore models, and coordination number in the percolation model were calculated. When coke produces significant changes in catalyst morphology, the tortuosity factor almost doubles its initial value for a coke content of 20%. On the contrary, the percolation model seems to predict changes accurately in porosity, mass transport coefficient, and an isolated porosity growing from the coordination number matched for a fresh catalyst.

Introduction

In most heterogeneous catalytic reactions where organic compounds are involved, for example, in petroleum refining and the petrochemical industry, catalyst deactivation due to coke deposits becomes an important problem to be considered (Wolf and Alfani, 1982; Hughes, 1984; Froment and Bischoff, 1990).

Coke is employed in literature referring to the end product of carbon disproportionation, condensation and hydrogen abstraction reactions of adsorbed carbon-containing species whose general composition is CH_n with standard n values ranging from 1 (Appleby et al., 1962) to 0.1 (Brodskii et al., 1976). Coke can produce site coverage which is responsible for a direct loss of active surface. Furthermore, a high coke content can block the access to the active sites, isolated zones appearing which can produce an important loss of active surface (Levinter et al., 1966) and a significant modification of the voidage and pore interconnections. Due to these facts, effective diffusivity can be drastically affected. This coefficient is usually defined by applying the Fick equation:

$$N_i = -D_e \cdot \frac{dC_i}{dR} \tag{1}$$

Then, effective diffusivity can be calculated as

$$D_e = \bar{D} \cdot f \tag{2}$$

where $\bar{D}$ considering the transition regime, both molecular and Knudsen diffusion, can be calculated as

$$\frac{1}{D_i(r_p)} = \frac{1}{D_{iK}(r_p)} + \frac{1}{D_{ij}} \tag{3}$$

Parameter f in Eq. 2 is a correction factor to take into account the complex internal structure of the solid.

If the process conditions and the pellet size are such that the diffusional time scale is the dominant factor, then it be-

comes essential to take into account the changes in the connectivity of the void space. This can be done predicting $\bar{D}$ and f values with coke content by means of a model for catalyst structure. Different levels of complexity have been used to describe the orientation, size and interconnection of the pores. Among the models proposed in literature two main groups can be distinguished:

(a) Models based on capillary network range from a simple bundle of cylindrical capillaries of uniform cross section (Wheeler, 1951, 1955) to the more sophisticated random pore model or cross-linked pore model (Johnson and Stewart, 1965). In the first model the value of r_p can be considered as an average of the values from different pore sizes calculated as:

$$\bar{r}_p = \frac{2 \cdot V_p}{S_g} \tag{4}$$

Therefore $\bar{D}$ is obtained from Eq. 3 with the r_p value from Eq. 4 to obtain Knudsen diffusivity value. In the second case, when a pore-size distribution $f(r_p)$ is considered, which is more realistic, the value of $\bar{D}$ is obtained as:

$$\bar{D}_i = \int_0^{\infty} \left(\frac{1}{\frac{1}{D_{iK(r_p)}} + \frac{1}{D_{ij}}} \right) \cdot f(r_p) \cdot dr_p \tag{5}$$

where $f(r_p)$ is a standard pore radius distribution which can be obtained from the gradient of cumulative pore volume curve.

Parameter f in Eq. 2 includes a tortuosity factor required to match the predictions to experimental data (Johnson and Stewart, 1965; Satterfield and Cadle, 1968; Feng and Stewart, 1973):

$$f = \frac{\epsilon}{\tau} \tag{6}$$

(b) The second main group is the *stochastic models* considering a randomly disordered media of void and solid zones. In this category a special mention can be made about the application of percolation concepts (Broadbent and Hammersley, 1957) to describe the porous matrix and associated transport properties (Mohanty et al., 1982; Reyes and Jensen, 1985; Shah, 1985). In the percolation theory *accessible porosity* ϵ^A is defined as the likelihood that any pore region is sufficiently well connected to the rest of those available for transport, and *total porosity* ϵ is the sum of accessible porosity and porosity in isolated pores ϵ^I. When porosity decreases due to coke growth inside the void space, a sharp decrease in accessible porosity and transport coefficients can appear if ϵ reaches a value close to percolation threshold. ϵ^c, under which pore space remains as disconnected regions or isolated pores with no possible mass transport inside the catalyst.

Evaluation of ϵ^A, ϵ^I, ϵ^c and f can be done employing the Bethe network as a model of pore space topology (Larson et al., 1981; Mohanty et al., 1982; Reyes and Jensen, 1985) (see Appendix). In the Bethe network a coordination number Z is defined as the number of bonds connected to a hypothetical site located at the center of a branching pore, averaged over all sites.

When coke grows inside the catalyst pellet, both terms in Eq. 2 affecting D_e are modified. The coefficient $\bar{D}$ changes if the pore radius changes and the factor f is modified because coke produces a decrease in catalyst porosity. The volume of coke in the pellet can be calculated as (Chang and Crynes, 1986):

$$V_c = \frac{\rho_{po}}{\rho_c} \cdot C_c \left(\frac{\text{cm}^3 \text{ coke}}{\text{cm}^3 \text{ catalyst}} \right) \tag{7}$$

and, hence, the total porosity remaining can be predicted as:

$$\epsilon = \epsilon_o - V_c \tag{8}$$

The parameters τ and Z must be determined from matching effective diffusion coefficients obtained experimentally at each $\%C_c$. Stochastic models (as the percolation model) seem to have the advantage of a constant Z with porosity changes (Reyes and Jensen, 1986a,b) while in pore models dependence of τ values with porosity has been found in the literature (Wakao and Smith, 1962; Satterfield, 1980), with τ merely an adjustable parameter with no well defined meaning.

Most of the works in literature dealing with effect of coke in catalyst structure can be classified mainly as experimental or theoretical approaches but prediction of results experimentally found from a solid structure model is still a goal to be reached. Among the experimental works which can be cited are those by Richardson (1972) who found no significant changes in effective diffusivity of a Co-Mo-Al_2O_3 catalyst until 13% coke content was reached; Butt et al. (1975), who measured effective diffusivities in zeolites, found that it halved when the coke content reached 4%; Thakur and Thomas (1984) found that the hydrotreating catalyst employed showed a significant reduction in pore volume and surface area for coke levels around 20%; Stiegel et al. (1985) observed a negligible decrease in the pore volume and no significant changes in internal surface area when the coke content is around 9%; Ammus et al. (1987) reported a loss of half the pore volume and inner surface area when the coke content was raised from 20 to 35%; Al-Bayaty et al. (1994) discovered that for silica-alumina, the effective diffusivity measured of zeolites and chromia-alumina catalysts decreased between 20 and 30% when increasing the coke content to 12%.

On the other hand, representative of theoretical developments describing catalyst structure evolution with coke content, mentioned work should include Tsakalis et al. (1984), Chang and Crynes (1986); and Prasad et al. (1986) who employ the Wheeler pore model: Mann et al. (1985) and Mann and Thomson (1987) who apply the parallel bundle pore model with pore volume distribution; Beeckman and Froment (1982) who developed an approach based upon a probability theory to predict τ; Sahimi and Tsotsis (1985), Shah and Ottino (1987), Melkote and Jensen (1989) and Beyne and Froment (1990) who employed the concepts of percolation theory to describe the catalyst network.

Table 1. Catalyst Properties at Different Coke Contents

Cat.	$\%C_c$(g/g) $(W_f - W_i)/W_i \times 100$	Coke Compos. (% Wt.) C	H	V_p cm³/g	S_g m²/g	ρ_p g/cm³	ϵ Exp.	ϵ^I Exp.	$\bar{r}_p$(Å) = $= \int r_p f(r_p) dr_p$
P1	0	–	–	1.69	150	0.550	0.93	0	300
P2	3.6	89.3	10.71	1.62	143	0.567	0.92	0.002	280
P3	13	90.9	9.10	1.41	132	0.622	0.88	0.022	260
Coke (from P)	–	91	9	0.139	44	2.57	0.36	–	63
C1	0	–	–	0.338	106	1.59	0.537	0.	50
C2	5	87.2	12.8	0.324	102	1.60	0.52	0.	50
C3	9	89.3	10.7	0.300	95	1.65	0.495	0.001	48
C4	15	90.9	9.09	0.24	86	1.80	0.44	0.029	46
C5	20	93.4	6.60	0.18	75	1.91	0.345	0.101	45
Coke (from C)	–	96	4	0.04	13.31	3.5	0.14	–	55

In this work two types of catalysts (Pt-Al_2O_3 and Ni-Mo-Al_2O_3) obtained from industrial plants after reaching significant coke levels are employed to experimentally determine the effective diffusion coefficient by means of the chromatographic technique. One model from each of the types mentioned above have been used; a random pore model and the stochastic model proposed by Reyes and Jensen (1985) based on percolation notions are applied to obtain from the effective diffusivity the corresponding τ and Z values. The dependence of both of these parameters with coke content has been analyzed. Both models quoted above will be employed to predict porosity and effective diffusivity evolution with increasing coke content and a comparison of these estimated values with the experimentally determined values will be accomplished.

Experimental

Materials

Catalysts employed are Pt-Al_2O_3 (hereafter abbreviated to *P*) and Ni-Mo-Al_2O_3 (hereafter abbreviated to *C*), both fresh and aged obtained from processes carried out in industrial plants. *P* catalyst (0.42% Pt, 99, 54% Al_2O_3) has been used in dehydrogenation of *n*-paraffins (C_{10}–C_{13}) in the gas phase in a fixed-bed reactor at temperatures between 400 and 500°C and a pressure range between 2 and 30 atm. Pellets are spheres of 0.16 cm in diameter. *C* catalyst (3.9% NiO, 7.7% P_2O_5, 20.8% MoO_3, 66.4% Al_2O_3) has been employed in hydrodesulfuration of light gas oil at temperatures between 300 and 400°C and pressures ranging from 10 to 60 atm. The reaction was carried out in a pseudo-trickle bed reactor. Pellets are cylinders with an equivalent spherical diameter of 0.14 cm. The reactants were fed clean of metal compounds and hence deactivation was only due to coke formation. First a devolatilization of adsorbed compounds was undertaken at 200°C under an inert atmosphere (N_2) for 3 h. Table 1 shows the properties of the fresh and aged catalysts employed after devolatilization. Specific surface was determined by the B.E.T. method using a Micromeritics Accusorb 2000 Sorptometer. Pore-size distribution, macro and microporosity, were measured using a mercury porosimeter Carlo Erba Milestone 2000 and a Coulter Omnisorb 100 Sorptometer. Coke contents in the catalysts studied were measured by an elemental analyzer LECO HCN 6000. In Table 1 are also listed the properties of coke extracted from both aged catalysts (*P* and *C*). Surface area, pore volume and coke content measurements were repeated four times for each sample shown in Table 1, and values obtained were averaged, the experimental error being related to such averaged values being lower than 6%.

Both catalysts studied (*P* and *C*) show an unimodal pore-size distribution and no significant changes of mean radius take place with increasing coke content, as can be seen in Figures 1a and 1b and properties listed in Table 1. On the other hand, cumulative pore volume shows a remarkable decrease when coke content is over 15%. Differences between the experimental porosity at each $\%C_c$ content and the porosity as predicted by Eq. 8 have been calculated, taking the ϵ_o value in Eq. 8 as the experimental measured porosity at $\%C_c = 0$, attributable to experimental isolated regions in the void zones ϵ^I_{exp}, which are also listed in Table 1. Note that for *C* catalysts, these isolated regions show an exponential increase for $\%C_c > 10\%$, while for Pt-Al_2O_3 at the maximum coke level reached (13%) isolated zones are still negligible. The *C/H* relationship obtained is in the range found in literature for this kind of process (Ocampo et al., 1978; Steigel et al., 1985; Ammus et al., 1987) and increases with increasing coke content (Diez and Gates, 1990).

Setup for effective diffusion coefficient measurements

The chromatographic technique in a packed column has been employed. A copper column 205 cm in length and 1.07 cm in internal diameter filled with the catalyst pellets has been used inside an oven, with a Hewlett-Packard 5710 A chromatograph with an on-line TC detector on line (the bed porosity resulting between 0.4 and 0.5). A six way valve permits an injection of 0.5 cm^3 of argon as tracer into the carrier stream (helium). The setup is explained in detail elsewhere (García-Ochoa and Santos, 1994).

Effective diffusion coefficient evaluation by chromatographic measurements

The flow inside the packed column is assumed to be isobaric and isothermal. In these conditions, the model of Kubin (1965) and Kucera (1965) can be applied to describe the mass transport inside the solid particle and through the packed

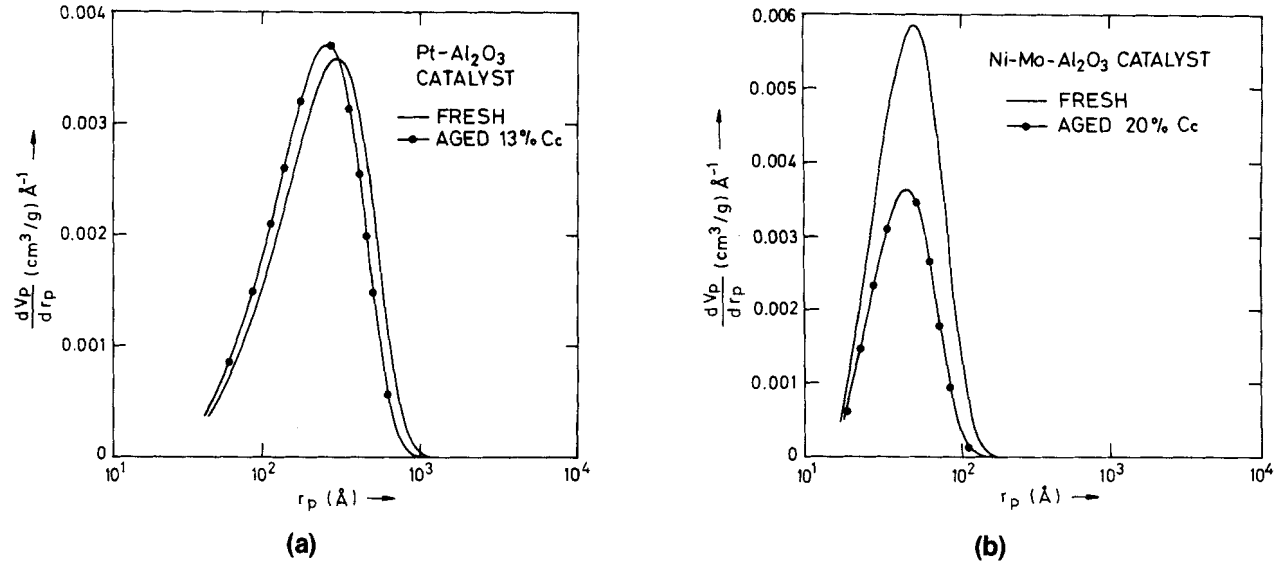

Figure 1. Pore volume distribution.

For $Pt\text{-}Al_2O_3$ fresh and aged (a); for $Ni\text{-}Mo\text{-}Al_2O_3$ fresh and aged (b).

bed. Because the tracer concentration in the gas phase is small, the physical adsorption rate can be considered as first-order. In this way, the model takes into account different phenomena in the pellet, such as adsorption and interphase and intra-phase diffusion, and axial dispersion in the bed, using the corresponding kinetic parameters: k_f, D_e, K_a and D_{ax}, respectively. By application of the Laplace transform to the differential equations of the Kubin (1965) and Kucera (1965) model, the moments of the tracer concentration-time curve can be calculated. Assuming that the adsorption-desorption equilibrium is reached, the two first moments of the tracer concentration-time curve have been determined as in a previous work (García-Ochoa and Santos, 1994) and the HEPT value can be calculated as:

$$\text{HEPT} = \frac{(\mu_2 - \mu_1^2)\cdot L}{\mu_1^2} = \frac{\sigma^2 \cdot L}{\mu_1^2} \tag{9}$$

with the relationship between HEPT and u_i, similar to that found by Van Deemter et al. (1956):

$$\text{HEPT} = \frac{A}{u_i} + B + G\cdot u_i \tag{10}$$

being the coefficient G of Eq. 10 (McGreavy and Siddiqui, 1980):

$$G = \frac{\frac{2}{15}\cdot\frac{\epsilon_L}{(1-\epsilon_L)}\cdot R_p^2}{\left(1+\frac{1}{\delta_o}\right)^2}\cdot\left(\frac{1}{D_e}+\frac{5}{k_f\cdot R_p}\right) \tag{11}$$

The adsorption equilibrium constant K_a has been calculated by linear regression of μ_1 vs. L/u_i (McGreavy and Siddiqui, 1980). The effective diffusivity D_e is obtained from G values, which are achieved by Eqs. 9 and 10, from HEPT values at different values of u_i. For D_e calculation from G values using Eq. 11, it is necessary to estimate k_f values by some of the equations given in the literature. In this work, the one proposed by Wakao et al. (1958) has been used:

$$\frac{2\cdot k_f\cdot R_p}{D_{ij}} = 2.00 + 1.45\cdot Re_p^{1/2}\cdot Sc^{1/3} \tag{12}$$

for $Re_p < 100$

Experimental Results

Experiments have been carried out at 473 K of temperature and 0.93 atm., with a carrier flow ranging from 500 to 1,900 cm^3/min (at 298 K) under isobaric conditions. A portion of the column outlet stream was vented to carry to the detector a flow between 50 and 100 cm^3/min. Because of the high velocities employed, a calming section consisting of a tube of 12 m in length and 0.7 cm of internal diameter was placed before the column for preheating of the carrier gas to the oven temperature setpoint. Eight groups of experiments have been carried out, three of them corresponding to fresh (P1) and two to different aged (P2 and P3) $Pt\text{-}Al_2O_3$ catalysts, and the other five were carried out with $Ni\text{-}Mo\text{-}Al_2O_3$ catalysts fresh (C1), partially deactivated at four coke contents (C2 to C5). In each of the groups above quoted interstitial velocity of the carrier has been changed from 20 to 70 cm/s.

For each run, carried out at a gas carrier velocity, the signal obtained in the TC detector was stored in an on-line computer and values of first μ_1 and second central moment σ^2 were obtained numerically from effluent concentration curve. Then HEPT values are calculated using Eq. 9. A relative influence of axial dispersion is found at the lower gas velocity range used. At the same time the velocity increases and HEPT becomes linear with u_i, being the internal diffu-

Table 2. Experimental Results Obtained from Chromatographic Measurements

Cat.	$\%C_c$ g/g	R_p cm	K_a	G (s)	$D_e \times 10^3$ cm^2/s
P1	0	0.08	≈ 0	0.0150	13.1
P2	3.6	0.08	≈ 0	0.0149	12.8
P3	13	0.08	≈ 0	0.0151	12.6
C1	1.95	0.07	≈ 0	0.017	5.06
C2	5	0.07	≈ 0	0.019	4.34
C3	9	0.07	≈ 0	0.024	3.25
C4	15	0.07	≈ 0	0.023	2.73
C5	20	0.07	≈ 0	0.030	1.50

sion the main mass transport resistance to consider, at the range of velocity employed.

The K_a values are calculated from μ_1. The values of parameter G can be obtained, according to Eq. 10 by using nonlinear regression (Marquardt, 1963), estimating k_f, R_p values by Eq. 12 and then calculating D_e according to Eq. 11. Experimental results obtained for K_a and D_e are given in Table 2. As can be seen, the adsorption constant of Ar at 200°C for all the catalysts studied is almost negligible, with a value close to 0. Hence, Ar can be assumed to be a nonadsorbable tracer at the temperature used (473 K). Experimental values of D_e have been interpreted according to Eq. 2 by means of a model of solid structure to reach the corresponding structural parameter, τ or Z. Models considered are the three described in the introduction: the bundle pore model, the cross-linked pore model and the percolation model, as representative of the two groups quoted above.

Bundle pore model

In this case $\overline{D}$ is evaluated by means of Eq. 3 and $\bar{r}_p$ is the mean pore radius obtained by Eq. 4 when the experimental values of S_g and V_p (Table 1) for each catalyst and level of coke reached are substituted. Values of molecular and Knudsen diffusion appearing in Eq. 3 have been estimated for the Ar-He system at 200°C and 0.93 atm, giving $D_{\text{Ar-He}} = 1.729$ and $D_k = 33{,}377 r_p$, both with units of cm^2/s, with r_p in cm.

Estimating $\overline{D}$ according to the procedure described above, the parameter f has been calculated from measured D_e values using Eq. 2, and then, the tortuosity factor τ has been obtained applying Eq. 6, by substituting ϵ for the corresponding experimental porosity data listed in Table 1. The results obtained for $\overline{D}$, f and τ are given in Table 3.

Cross-linked pore model

In this case, coefficient $\overline{D}$ is evaluated from Eq. 5, where $f(r_p)$ is taken as the experimental pore-size distribution found for the catalyst and coke content considered. For each pair of D_e and $\overline{D}$ data, f and τ values are calculated as in the bundle pore model. The results obtained are listed in Table 3.

Percolation model

In the same way as in the cross-linking pore model, coefficient $\overline{D}$ is calculated from Eq. 5 introducing the corresponding pore-size distribution found experimentally. The f values are then calculated from Eq. 2. In this model, accessible porosity (which would correspond to that measured experimentally) and total porosity (which is not a directly measured variable) are distinguished, both porosities being connected by means of the percolation number value Z. Total porosity (ϵ_o) and coordination number (Z) for both fresh catalysts considered have been calculated from f values obtained with fresh catalysts and employing the respective accessible porosities listed in Table 1, by means of Eqs. A1 to A7 of the Appendix. As can be seen from the results listed in Table 4 in the case of Pt-Al_2O_3 catalyst, the meaningless coordination number value $Z < 3$ is obtained, and thus the percolation model should not be applied for this catalyst. On the other hand, for fresh Ni-Mo-Al_2O_3 catalyst ($C1$) a coordination number of 4 and a total initial porosity of 0.56 is obtained. For Ni-Mo-Al_2O_3 catalysts partially deactivated ($C2$ to $C5$), total porosity at the respective coke content (ϵ) is calculated from total porosity evaluated for the fresh catalyst ($\epsilon_o = 0.56$) according to Eq. 8. Accessible porosity ϵ^A and correction factor f are predicted for each $\%C_c$ according to Eqs. A2, A3, A5, A6 and A7, substituting the corresponding ϵ value and employing the coordination number evaluated for fresh catalyst ($Z = 4$). Finally, isolated porosity is calculated as the difference from total porosity and accessible porosity predicted.

Table 4 shows the predicted values of ϵ^A, ϵ^I and f together with those experimentally found; a good agreement can be observed for both types of data. Figure 2 shows the ϵ^A and f values as a function of ϵ, having the coordination number Z as parameter.

Discussion

Regarding the results obtained from D_e values measured by chromatographic technique employing a Pt-Al_2O_3 (P) at

Table 3. Parameter f and τ Values Obtained Applying Bundle Pore Model and Cross-Linked Pore Model to D_e Experimental Data

	Bundle Pore Model						Cross Linked Pore Model					
Cat.	$\bar{r}_p$ Å	ϵ_{ex}	$\overline{D}$ cm^2/s	D_e cm^2/s	f	τ	ϵ_{ex}	$\overline{D}$ cm^2/s	D_e cm^2/s	f	τ	$\bar{r}_p$ Å
P1	221	0.93	0.0705	0.0132	0.186	5	0.93	0.1130	0.0132	0.117	8.0	300
P2	226	0.92	0.0724	0.0128	0.176	5.2	0.92	0.1070	0.0128	0.120	7.7	280
P3	229	0.88	0.0730	0.0126	0.172	5.1	0.88	0.0995	0.0126	0.127	6.9	260
C1	64	0.537	0.0211	0.00506	0.24	2.2	0.537	0.0200	0.00506	0.25	2.1	50
C2	63	0.520	0.0211	0.00434	0.21	2.5	0.520	0.0200	0.00434	0.22	2.2	50
C3	63	0.495	0.0211	0.00325	0.155	3.2	0.495	0.0191	0.00325	0.171	2.9	48
C4	56	0.440	0.0183	0.00273	0.149	2.9	0.440	0.0181	0.00273	0.151	2.9	46
C5	48	0.345	0.0158	0.00150	0.094	4.8	0.345	0.0181	0.00150	0.083	4.1	45

Table 4. Coordination Number, Z, f and ϵ^A Values Obtained for Fresh and Aged Catalysts Applying Percolation Model

Cat.	ϵ^A	$\bar{D}$ (cm²/s)	D_e (cm²/s)	f	Z	ϵ^{TOTAL}
P1	0.93	0.113	0.0132	0.117	< 3	0.93
C1	0.537	0.020	0.0056	0.25	4	0.555

Cat.	ϵ_o	$\%C_c$ (g/g)	V_c Eq. 15	ϵ^A Exp.	ϵ^A $Z=4$	$\bar{D}$ (cm²/s)	$D_e \cdot 10^3$ (cm²/s)	f Exp.	f $Z=4$	ϵ^I $Z=4$
C1	0.56	0.05	0.023	0.52	0.51	0.020	4.34	0.22	0.24	0.03
C2	0.56	0.09	0.041	0.49	0.49	0.019	3.25	0.17	0.20	0.03
C3	0.56	0.15	0.068	0.44	0.45	0.018	2.73	0.15	0.17	0.04
C4	0.56	0.20	0.091	0.35	0.39	0.018	1.5	0.08	0.12	0.12

different coke levels, it is found that even at the maximum coke content present in this catalyst (13%) no remarkable changes in pore structure, internal surface and porosity are found, as can be seen in Table 1. This is in agreement with the close effective diffusion coefficient values obtained employing fresh and aged catalyst. Because of such high initial porosity of this catalyst (0.93), the percolation model does not seem useful to describe pore topology and its evolution with coke growth, resulting in a coordination number less than 3 (Table 4). This means no branched pores and consequently an unrealistic situation. The high initial porosity of Pt-Al_2O_3 catalyst means that it is highly connected and clearly the Bethe network results are inappropriate. The reason why no isolated regions are present in this catalyst can be due to the fact that in the region far from umbral percolation value ϵ^c, the decreasing of porosity by coke fouling is almost the same as the coke volume in the pellet. Application of both pore models (bundle pore model and cross-linked model) to fresh Pt-Al_2O_3 catalyst yields reliable tortuosity values, resulting in a value of τ around 5 in the bundle pore model and about 8 in the cross-linked pore model. The τ value remains, as could be expected from the above, almost unchanged for Pt-Al_2O_3 aged catalysts, as can be seen in Table 3.

On the other hand, when results obtained with Ni-Mo-Al_2O_3 catalyst (initial porosity 0.53) are analyzed, it can be pointed out that when the coke content is about 20%; inner surface and porosity are reduced by around 30% and 40%, respectively, in relation to those values found for fresh Ni-Mo-Al_2O_3 catalyst (see Table 1). This is in agreement with the literature for hydrotreating catalysts suffering coke deactivation: Thakur and Thomas (1984) who find a decrease of 50% in pore volume and inner surface for coke levels up 20%; Stiegel et al. (1985), who find a reduction of about 15% for pore volume and no significant changes in internal surface when coke is around 9%; Ammus et al. (1987), who relate a loss of 50% of pore volume and inner surface when coke content is in the range from 20 to 35%.

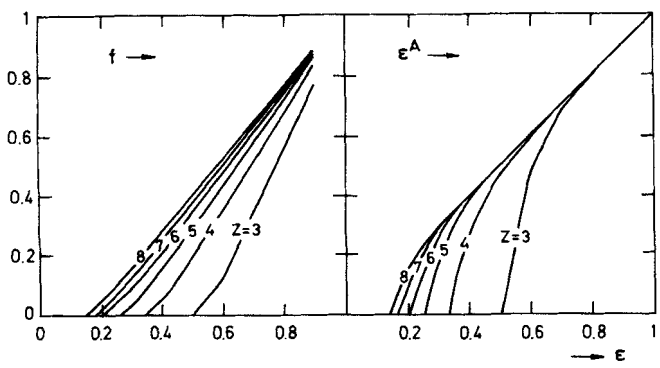

Figure 2. ϵ^A and f values as a function of ϵ, Z as parameter.

In the Ni-Mo-Al_2O_3 catalyst, isolated pore regions become significant for coke levels of 15%, which is associated to a sharp decrease in effective diffusion coefficient at this level of coke content (Table 2). This has also been observed by Richardson (1972), who found that D_e values measured by the chromatographic technique using several Co-Mo-Al_2O_3 aged catalyst remain almost unchanged up to a coke level of around 13%, with a sharp decrease when coke content goes over that value.

Bundle pore models and cross-linked pore models predict values of tortuosity factors continuously increasing with rising coke content with this increase being especially remarkable when the coke content goes to 15%, where τ becomes almost double with respect to the value obtained for fresh catalyst and no isolated porosity (experimentally measured) is considered in the models quoted above. Nevertheless, the coordination number Z calculated by means of percolation model for fresh Ni-Mo-Al_2O_3 catalyst, is able to accurately predict the evolution of effective diffusion coefficient (Table 4), with coke content increase and the growth of isolated pore zones. Therefore, the percolation model seems to be suited more to describe the catalyst topology when this behaves as a dynamic network with significant changes of structural properties, as is the case of catalyst deactivation when coke deposit reaches significant levels in the pellet.

The level of coke for which remarkable changes in intraparticle mass transport take place depends on the nature of reaction and initial structure of catalyst considered. Thus, for catalysts with porosity close to the threshold level, the coke content producing changes in the intraparticle mass transport rate should be lower than that for catalysts with higher porosity. Furthermore, another point which should be analyzed in the deactivation of catalysts reaching high enough coke levels is the prediction of changes in pore-distribution size with increasing coke content. The percolation model does not account for the preferential plugging of the narrowest pores postulated in coke deactivation, and this is a limitation that should also be considered. The problem of pore distribution changes has been the subject of theoretical works without experimental confirmation (Mann et al., 1985; Chang and Crynes, 1986; Mann and Thomson, 1987).

Acknowledgment

This work has been supported by D.G.I.C.Y.T. under contract no. PB89-0118. The authors wish to thank Research Center of CEPSA

for supplying the catalyst and their kind help in some of the measurements of the catalyst properties.

Notation

A = parameter in Eq. 10
B = parameter in Eq. 10
C = concentration (mol/L)
$C_{1\ldots5}$ = Ni-Mo-Al_2O_3 catalyst at different coke levels
$\%Cc$ = percentage catalyst coke content, g/g
$\bar{D}$ = average composite local diffusivity value, cm^2/s
$D(r_p)$ = composite diffusivity value, cm^2/s
D_{ax} = axial dispersion coefficient, cm^2/s
D_e = effective diffusivity, cm^2/s
D_{ij} = molecular diffusivity, cm^2/s
D_{iK} = Knudsen diffusivity, cm^2/s
f = structural correction factor in Eq. 2, defined by Eq. 6, A5 or A6
$f(r_p)$ = pore radius distribution function, cm^{-1}
G = parameter in Eq. 10, defined by Eq. 11
HEPT = equivalent height of theoretical plate, cm
k_f = interphase mass-transfer coefficient, cm/s
L = chromatographic packed column length, cm
M = molecular weight
N = diffusion rate, $mol/cm^2 \cdot s$
P = pressure, atm
$P_{1\ldots3}$ = Pt-Al_2O_3 catalyst at different coke levels
q = carrier gas flow, cm^3/min
r_p = pore radius, cm, A
R_p = particle radius, cm
Re_p = particle Reynolds number
Sc = Schmidt number
S_g = specific surface, m^2/g
T = temperature, K
u_i = interstitial velocity, cm/s
u_L = gas linear velocity, cm/s
V_c = volume of coke deposit, cm^3 coke/cm^3 catalyst
V_p = pore volume, cm^3/g
W_f = weight of aged catalyst, g
W_i = weight of fresh catalyst, g

Greek letters

ϵ = porosity
ϵ^R = root of polynomial in Eq. A3
μ_1 = first absolute moment of tracer response, s
$\mu_{1,2}$ = first and second moments of tracer responses, s, s^2, respectively
ρ_c = coke density, g/cm^3
ρ_p = pellet density, g/cm^3
σ^2 = second central moment or variance of tracer response, s^2
τ = tortuosity factor

Subscripts

a = related to adsorption in catalyst surface
ax = relative to the axial dispersion in the bed
c = relative to coke
f = relative to interphase
i = for Compound i
j = for Compound j
L = relative to the bed
o = for fresh catalyst
p = for pellet or pore

Literature Cited

Al-Bayati, S., D. R. Acharya, and R. Hughes, "Effect of Coke Deposition on the Effective Diffusivity of Catalyst Pellets," *Appl. Catal. A. General*, **110**, 109 (1994).

Ammus, J. M., G. P. Androutsopoulos, and A. H. Tsetsekou, "An Investigation of the Deactivation Phenomena Associated with the Use of Commercial HDS Catalysts," *Ind. Eng. Chem. Res.*, **26**, 1312 (1987).

Appleby, W. G., J. W. Gibson, and G. M. Good, "Coke Formation in Catalytic Cracking," *Ind. Eng. Chem. Process Des. Dev.*, **1**, 102 (1962).

Beeckman, J. W., and G. F. Froment, "Deactivation of Catalysts by Coke Formation in the Presence of Internal Diffusional Limitation," *Ind. Eng. Chem. Fund.*, **21**, 243 (1982).

Beyne, A. O. E., and G. F. Froment, "A Percolation Approach for the Modeling of Deactivation of Zeolite Catalysts by Coke Formation," *Chem. Eng. Sci.*, **45**, 2089 (1990).

Broadbent, S. R., and J. M. Hammersley, "Percolation Processes I: Crystal and Mazes," *Proc. Camb. Phil. Soc.*, **53**, 629 (1957).

Brodskii, E. S., I. M. Lakashenko, and V. G. Lebedevskaya, "Use of Mass Spectrometry Data and Physicochemical Characteristics for the Analysis of Petroleum Fractions," *Chem. Abstr.*, **85**, 35292d, *Neftekhimiya*, **16**, 138 (1976).

Butt, J. B., S. Delgado Díaz, and W. E. Muno, "Effects of Coking on the Transport Properties of H-Mordenite," *J. Catal.*, **37**, 158 (1975).

Chang, H. J., and B. L. Crynes, "Effect of Catalyst Pore and Pellet Sizes on Deactivation in SRC Oil Hydrotreatment," *AIChE J.*, **32**, 224 (1986).

Díez, F., and B. C. Gates, "Deactivation of a Ni-Mo/γAl_2O_3 Catalyst: Influence of Coke on the Hydroprocessing Activity," *Ind. Eng. Chem. Res.*, **29**, 1999 (1990).

Feng, C., and W. E. Stewart, "Practical Models for Isothermal Diffusion and Flow of Gases in Porous Solids," *Ind. Eng. Chem. Fundam.*, **12**, 143 (1973).

Froment, G. F., and K. B. Bischoff, "Chemical Reactor Analysis and Design," 2nd ed., Wiley, New York (1990).

García-Ochoa, F., and A. Santos, "Effective Diffusivity Under Inert and Reaction Conditions," *Chem. Eng. Sci.*, **49**, 3091 (1994).

Hughes, R., *Deactivation of Catalysts*, Academic Press, New York (1984).

Johnson, M. F. L., and W. E. Stewart, "Pore Structure and Gaseous Diffusion in Solid Catalysts," *J. Catal.*, **4**, 248 (1965).

Kubin, M., "Theory of the Chromatography: II. Effect of the External Diffusion and of the Adsorption in the Sorbent Particle," *Coll. Czech. Chem. Commun.*, **30**, 2900 (1965).

Kucera, E., "Theory of Chromatography. Linear Nonequilibrium Elution Chromatography," *J. Chromatog.*, **19**, 237 (1965).

Larson, R. G., L. E. Scriven, and H. T. Davis, "Percolation Theory of Two-Phase Flow in Porous Media," *Chem. Eng. Sci.*, **36**, 57 (1981).

Levinter, M. E., G. M. Panchenkov, and A. Tanatarov, "Chain Mechanism of the Poisoning of Aluminosilicate Catalyst by Amines," *Chem. Abstr.*, **65**: 16843c, *Zh. Fiz. Khim.*, **40**, 1632 (1966).

Mann, R., and G. Thomson, "Deactivation of a Supported Zeolite Catalyst: Simulation of Diffusion, Reaction and Coke Deposition in a Parallel Bundle," *Chem. Eng. Sci.*, **2**, 555 (1987).

Mann, R., F. Y. A. El-Kady, and R. Marzin, "Catalyst Deactivation by Fouling: A Wedge-Layering Analysis of the Consecutive Reaction," *Chem. Eng. Sci.*, **40**, 249 (1985).

Marquardt, F. W., "An Algorithm for Least-Squares Estimation of Nonlinear Parameters," *J. Soc. Ind. Appl. Math.*, **2**, 431 (1963).

McGreavy, C., and M. A. Siddiqui, "Consistents Measurements of Diffusion Coefficients for Effectiveness Factors," *Chem. Eng. Sci.*, **35**, 3 (1980).

Melkote, R. R., and K. F. Jensen, "Models for Catalytic Pore Plugging: Application to Hydrometallation," *Chem. Eng. Sci.*, **44**, 649 (1989).

Mohanty, K. K., J. M. Ottino, and H. T. Davis, "Reaction and Transport in Disordered Composite Media: Introduction of Percolation Concepts," *Chem. Eng. Sci.*, **37**, 905 (1982).

Ocampo, A., J. T. Schrodt, and S. M. Kovach, "Deactivation of Hydrodesulfurization Catalysts under Coal Liquids. 1. Loss of Hydrogenation Activity Due to Carbonaceous Deposits," *Ind. Eng. Chem. Prod. Res. Dev.*, **17**, 56 (1978).

Prasad, K. B. S., R. Valdyeswaran, and M. S. Ananth, "Transient Analysis of Deactivation in a Single Pellet with Changing Diffusivity and Voidage," *Ind. Eng. Chem. Fundam.*, **25**, 184 (1986).

Reyes, S., and K. F. Jensen, "Estimation of Effective Transport Coefficients in Porous Solids Based on Percolation Concepts," *Chem. Eng. Sci.*, **40**, 1723 (1985).

Reyes, S., and K. F. Jensen, "Percolation Concepts in Modeling of Gas-Solid Reactions: I. Application to Char Gasification in the Kinetic Regime," *Chem. Eng. Sci.*, **41**, 333 (1986a).

Reyes, S., and K. F. Jensen, "Percolation Concepts in Modeling of Gas-Solid Reactions: II. Application to Char Gasification in the Diffusion Regime," *Chem. Eng. Sci.*, **41**, 345 (1986b).
Richardson, J. T., "Experimental Determination of Fouling Parameters," *Ind. Eng. Chem. Process Des. Dev.*, **11**, 12 (1972).
Sahimi, M., and T. Tsotsis, "A Percolation Model of Catalyst Deactivation by Site Coverage and Pore Blockage," *J. Catal.*, **96**, 552 (1985).
Santos, A., "Desactivación de Catalizadores por Coque," PhD Thesis, Univ. Complutense, Madrid (1992).
Satterfield, C. N., and P. J. Cadle, "Diffusion in Commercially Manufactured Pelleted Catalysts," *Ind. Eng. Chem. Process Des. Dev.*, **7**, 257 (1968).
Satterfield, C. N., *Heterogeneous Catalysis in Practice*, McGraw-Hill, New York (1980).
Shah, N., "Development and Application of Models for Transport and Reaction in Composite Media," PhD Thesis, Univ. of Massachusetts (1985).
Shah, N., and J. M. Ottino, "Transport and Reaction Envolving Disordered Composites: II. Coke Deposition in a Catalytic Pellet," *Chem. Eng. Sci.*, **42**, 73 (1987).
Stiegel, G. J., R. E. Tischer, D. L. Cillo, and N. K. Narain, "Catalyst Deactivation in Two-Stage Coal Liquefaction," *Ind. Eng. Chem. Prod. Res. Dev.*, **24**, 206 (1985).
Stimchombe, R. B., "Conductivity and Spin-Wave Stiffness in Disordered Systems: An Exactly Soluble Model," *J. Phys. Chem. Solid State Phys.*, **7**, 179 (1974).
Thakur, D. S., and M. G. Thomas, "Catalyst Deactivation during Direct Coal Liquefaction: A Review," *Ind. Eng. Chem. Prod. Res. Dev.*, **23**, 349 (1984).
Tsakalis, K. S., T. T. Tsotsis, and G. J. Stiegel, "Deactivation Phenomena by Site Poisoning and Pore Blockage: The Effect of Catalyst Size, Pore Size and Pore Distribution," *J. Catal.*, **88**, 188 (1984).
Van Deemter, J. J., F. J. Zuiderweg, and A. Klinkenberg, "Longitudinal Diffusion and Resistance to Mass Transfer as Causes of Non-Ideality in Chromatography," *Chem. Eng. Sci.*, **5**, 271 (1956).
Wakao, N., and J. M. Smith, "Diffusion in Catalyst Pellets," *Chem. Eng. Sci.*, **17**, 825 (1962).
Wakao, N., T. Oshima, and S. Yagi, "Mass Transfer from Packed Beds of Particles to a Fluid," *Kagaku Kogaku*, **22**, 780 (1958).
Wheeler, A., "Reaction Rates and Selectivity in Catalyst Pores," *Advances in Catalysis*, **Vol. 3**, W. G. Frankerburg et al., eds., Academic Press, New York (1951).
Wheeler, A., "Reaction Rates and Selectivity in Catalyst Pores," *Catalysis*, **Vol. 2**, P. H. Emmett, ed., Reinhold, New York (1955).
Wolf, E. E., and F. Alfani, "Catalyst Deactivation by Coking," *Catal. Rev. Sci. Eng.*, **24**, 329 (1982).

Appendix

Percolation threshold, accessible and isolated porosity: ϵ^c, ϵ^A and ϵ^I, respectively, can be calculated in the percolation model as:

$$\epsilon^c = \frac{1}{(Z-1)} \tag{A1}$$

$$\epsilon^A = \begin{cases} 0 & \text{for } \epsilon < \epsilon^c \\ \epsilon \cdot \left(1 - \left(\frac{\epsilon^R}{\epsilon}\right)^{\frac{(2Z-2)}{(Z-2)}}\right) & \text{for } \epsilon \geq \epsilon^c \end{cases} \tag{A2}$$

with

$$\epsilon^R \cdot (1-\epsilon^R)^{(Z-2)} - \epsilon \cdot (1-\epsilon)^{(Z-2)} = 0 \tag{A3}$$

$$\epsilon^I = \epsilon - \epsilon^A \tag{A4}$$

If the porosity value is close to ϵ^c then f can be obtained as (Stimchombe, 1974):

$$f = 1.522 \cdot \frac{(Z-1)^3}{(Z-2)^2} \cdot (\epsilon - \epsilon^c)^2 \tag{A5}$$

while when porosity is in the far-percolation region parameter f can be calculated as (Stimchombe, 1974):

$$f = -\frac{(Z-1)}{(Z-2)} \cdot \Sigma_0^\infty G_s \tag{A6}$$

with

$$G_0 = -(\epsilon - \epsilon^c)$$

$$G_1 = 0$$

$$G_2 = \left(\frac{\epsilon^c}{\epsilon}\right)^2 \cdot (\epsilon - \epsilon^c) \cdot (1-\epsilon)$$

$$G_3 = \frac{(\epsilon^c)^3}{\epsilon^5} (\epsilon - \epsilon^c)^2 \cdot (1-\epsilon) \cdot [\epsilon \cdot (2 \cdot \epsilon - 1) + 2 \cdot (\epsilon - \epsilon^c) \cdot (1-\epsilon)]$$

$$G_4 = \frac{(\epsilon^c)^4}{\epsilon^6} (\epsilon - \epsilon^c)^2 \cdot (1-\epsilon) \left[3 \cdot (1-\epsilon)^2 \cdot (\epsilon - \epsilon^c) - 2 \cdot \epsilon \cdot (1-\epsilon) + (\epsilon - \epsilon^c) \cdot (1 - 3 \cdot \epsilon + 3 \cdot \epsilon^2) + 5 (\epsilon - \epsilon^c)^2 \cdot (1-\epsilon) \cdot \left(\frac{2 \cdot \epsilon - 1}{\epsilon}\right) + \frac{15}{\epsilon^2} (\epsilon - \epsilon^c)^3 \cdot (1-\epsilon)^2 \right] \tag{A7}$$

Manuscript received Apr. 18, 1994, and revision received Feb. 21, 1995.